Published OnlineFirst February 22, 2019; DOI: 10.1158/1541-7786.MCR-18-1306

Genome Maintenance

Molecular Cancer Research

The SIAH1–HIPK2–p53ser46 Damage Response Pathway is Involved in Temozolomide-Induced Glioblastoma Cell Death

Yang He, Wynand P. Roos, Qianchao Wu, Thomas G. Hofmann, and Bernd Kaina

Abstract

Patients suffering from glioblastoma have a dismal prognosis, indicating the need for new therapeutic targets. Here we provide evidence that the DNA damage kinase HIPK2 and its negative regulatory E3-ubiquitin ligase SIAH1 are critical factors controlling temozolomide-induced cell death. We show that HIPK2 downregulation (HIPK2kd) significantly reduces the level of apoptosis. This was not the case in glioblastoma cells expressing the repair protein MGMT, suggesting that the primary DNA lesion responsible for triggering HIPK2-mediated apoptosis is O^6-methylguanine. Upon temozolomide treatment, p53 becomes phosphorylated whereby HIPK2kd had impact exclusively on ser46, but not ser15. Searching for the transcriptional target of p-p53ser46, we identified the death receptor FAS (CD95, APO-1) being involved. Thus, the expression of FAS was attenuated following HIPK2kd, supporting the conclusion that HIPK2 regulates temozolomide-induced apoptosis via p-p53ser46-driven FAS expression. This was substantiated in chromatin-immunoprecipitation experiments, in which p-p53ser46 binding to the Fas promotor was regulated by HIPK2. Other pro-apoptotic proteins such as PUMA, NOXA, BAX, and PTEN were not affected in HIPK2kd, and also double-strand breaks following temozolomide remained unaffected. We further show that downregulation of the HIPK2 inactivator SIAH1 significantly ameliorates temozolomide-induced apoptosis, suggesting that the ATM/ATR target SIAH1 together with HIPK2 plays a pro-apoptotic role in glioma cells exhibiting p53wt status. A database analysis revealed that SIAH1, but not SIAH2, is significantly overexpressed in glioblastomas.

Implications: The identification of a novel apoptotic pathway triggered by the temozolomide-induced DNA damage O^6-methylguanine supports the role of p53 in the decision between survival and death and suggests SIAH1 and HIPK2 as new therapeutic targets.

Introduction

Malignant brain tumors, notably the most common and aggressive form glioblastoma multiforme, remain to date a therapeutic challenge. Therapy includes resection followed by radiotherapy and concomitant and adjuvant chemotherapy with temozolomide (TMZ). Even with this therapy regimen, the patient is faced with a bad prognosis, as the median length of survival of patients diagnosed with this cancer is 9.7–14.6 months (1, 2). Elucidation of the molecular pathways involved in the therapeutic response may identify possible targets for intervention, or at least lead to better predictors of outcome.

The first-line therapeutic drug, TMZ, is a methylating agent that targets, like other methylating anticancer drugs such as dacarbazine, procarbazine, and streptozotocin, nucleophilic centers in the DNA (3). Oral TMZ enters the systemic circulation and then crosses the blood–brain barrier. It enters the cells by diffusion and hydrolyses to 3-methyl-(triazen-1-yl)imidazole-4-carboxamide (MTIC). MTIC further decomposes to 4-amino-5-imidazole carboxamide generating methyl diazonium ions. These methylate DNA at multiple sites of which O^6-methylguanine (O^6MeG) is the clinically relevant killing lesion (4–6). O^6MeG is repaired by O^6-methylguanine-DNA methyltransferase (MGMT) in a suicide repair reaction that restores guanine, but inactivates the repair protein itself (7). The resistance of glioblastoma cells to TMZ and, consequently, the resistance of tumors in this therapeutic situation is therefore dependent on the amount of MGMT they express (8). The expression of MGMT is governed by epigenetic modification of CpG islands in its promotor (9). Methylation in these CpG islands silences the *MGMT* gene, which has been shown to be prognostic for glioblastoma therapy outcome (10, 11).

A key question in understanding the mechanism of TMZ (and other methylating anticancer drugs) is how the small (and mutagenic) DNA damage O^6MeG triggers cell death. There is compelling evidence that O^6MeG lesions induced by TMZ are converted into DNA double-strand breaks (DSB) in a replication and mismatch repair (MMR) dependent manner (12–14). These DSBs activate the DNA damage response (DDR), which in turn trigger the stabilization of p53 and the p53-dependent transcriptional upregulation of several pro- and anti-apoptotic genes, including the death receptor FAS (alias CD95, APO-1; refs. 15, 16). In contrast, in p53-mutated cancer cells the mitochondrial pathway becomes activated, which is however less effective in inducing apoptosis and therefore requires higher DNA damage levels (15, 16). The pro-apoptotic effect of p53 in glioma cells is counteracted by the p53-p21–dependent prosurvival pathway

Institute of Toxicology, University Medical Center, Mainz, Germany.

Note: Supplementary data for this article are available at Molecular Cancer Research Online (http://mcr.aacrjournals.org/).

Corresponding Author: Bernd Kaina, Institute of Toxicology, Medical Center of the University Mainz, Obere Zahlbacher Str. 67, D-55131 Mainz, Germany. Phone: 0049-6131-17-9217; Fax: 0049-6131-17-8499; E-mail: kaina@uni-mainz.de

doi: 10.1158/1541-7786.MCR-18-1306

Published OnlineFirst February 22, 2019; DOI: 10.1158/1541-7786.MCR-18-1306

through cell-cycle arrest in G_2–M and presumably also upregulation of DNA repair (15–17). As the majority of glioblastomas retain functional p53 (18), the cellular responses triggered by this tumor suppressor protein are crucial in understanding of how glioblastoma cells respond to therapy.

Although appropriate studies are lacking for glioblastoma, the cell fate determining functions of p53 appear to be regulated by different posttranslational modifications of p53, leading to different promoter selectivity of this transcription factor (19). Thus, it has been shown that phosphorylation of p53 at serine 15 (p53ser15) by ATM and ATR (20) and serine 20 by the checkpoint kinases CHK1 and CHK2 (21) is vital for p53 stabilization, its transcriptional activation and binding, for example, to the promoter of p21 (22), whereas phosphorylation of p53 at serine 46 (p53ser46) triggers transactivation of pro-apoptotic target genes like p53AIP1 (23) or PTEN (24). Phosphorylation of p53 at Ser46 is not a direct consequence of checkpoint kinases (ATM, ATR, CHK1, CHK2), but is rather mediated by the homeodomain interacting protein kinase 2 (HIPK2), which was demonstrated being a new player in the DDR (25, 26). Thus, it has been shown in cells exposed to ultraviolet light, ionizing radiation (27), doxorubicin (28), and cisplatin (29) that p53 is a substrate of HIPK2 yielding p53ser46. The upstream activators of HIPK2 are the DDR kinases ATM (27, 30) and ATR (31), which phosphorylate the E3 ubiquitin-protein ligase seven in absentia homolog 1 (SIAH1), which was shown to interact with HIPK2 causing its degradation (31). Thus, upon SIAH1 phosphorylation, HIPK2 becomes stabilized and activated. Although the ATM/ATR–SIAH1–HIPK2 pathway has been well characterized (19, 32), it is still unclear whether it is a specific response evoked in only some cell types and upon treatment with specific genotoxins and whether it becomes activated also in brain cancer cells, for which data are lacking. It is also unknown whether the HIPK2 pathway gets activated by alkylating agents, like TMZ and chloroethylnitrosoureas, which are first- and second-line drugs in glioblastoma therapy. Also the questions as to the type of DNA damage that triggers the response and the HIKP2 stimulated pro-apoptotic functions in glioblastoma cells have not yet been addressed. Because alkylating agents are not only used in brain cancer therapy, the data bear important implications also for other tumor entities treated with alkylating therapeutics.

In this study, we examined the influence of HIPK2 and its inhibitor, SIAH1, on the resistance of glioblastoma cells to the methylating agent TMZ and the chloroethylating nitrosourea lomustine (CCNU). The data show that HIPK2 ameliorates TMZ, but not CCNU-induced apoptosis. Furthermore, we show that the DNA lesion O^6MeG, which gives rise to MMR-mediated DSB (14) leading to ATR/ATM activation (33), stimulates HIPK2 and phosphorylation of p53 at serine 46. This augments binding of p53 to the *FAS (CD95/Apo-1)* promoter, transcription of the gene, and activation of the apoptosis pathway. We further show that glioblastomas frequently overexpress the HIPK2 inhibitor SIAH1. In these tumors, the HIPK2 function is anticipated to be limited. We experimentally supported this hypothesis by knockdown of SIAH1, which caused HIPK2 accumulation and consequently sensitization of glioblastoma cells to TMZ-induced apoptosis. Because HIPK2 selectively affected the apoptotic response and its downregulation had no impact on TMZ-induced senescence and autophagy, our findings identified this kinase as a key regulator in the decision between survival and death through apoptosis in glioblastoma cells. Collectively, the data lend compelling support for a role of SIAH1 and the HIPK2-p53ser46 driven apoptotic pathway in TMZ-induced cell death and identified them as new therapeutic targets in malignant glioma therapy.

Materials and Methods

Cell lines and culture conditions

The human glioblastoma cell line LN-229 (RRID:CVCL_0393) was purchased from ATCC, the human glioma lines U87MG (RRID:CVCL_0022) and LN-308 (RRID:CVCL_0394) were from the laboratory of Prof. M. Weller (Molecular Neurooncology, University of Zurich, Switzerland), rechecked and described in our previous work (15, 16). Upon receipt, all cell lines were amplified for cryopreservation in liquid-N_2 and freshly thawed cell stocks were used for every battery of tests. LN-229, U87MG, LN-308, and the LN-229 line stably transfected with human MGMT cDNA (34) were cultured in DMEM supplemented with 10% FBS (Gibco; Life Technologies, Thermo Fisher Scientific). Cells were routinely checked for mycoplasma contamination and maintained at 37°C in a humidified 5% CO_2 atmosphere.

Generation of dominant-negative FADD and MGMT expressing cells, siRNA and transfection

The generation and maintenance of LN-229 cells stably overexpressing MGMT (LN-229MGMT) has been described previously (35). For the generation of LN-229 cells that stably overexpress and a dominant-negative form of FADD (DN-FADD), LN229 cells were transfected with the plasmid pcDNA3-DN-FADD (36) using the Effectene Transfection Kit (Qiagen). G418-resistant clones were picked, expanded, and tested for expression by Western blot analysis. Positive clones were routinely cultured in medium containing 0.75 mg/mL G418 (Sigma-Aldrich), which was omitted during the experiments.

For RNAi-mediated knockdown of HIPK2, siRNAs with the following sequences were used: siHIPK2-1 (5′-CCAGGTGAACATGACGACAGA-3′) and siHIPK2-2 (5′-AAGCGTCGGGTGAATATGTAT-3′) were from Qiagen. For knockdown of SIAH1 and SIAH2, siRNA for SIAH1 was from Dharmacon custom siRNA (GATAGGAACACGCAAGCAA) and SIAH2 siRNA was from Dharmacon siGenome SMARTpool. For knockdown of DcR1, siRNA (sc-40235) was from Santa Cruz Biotechnology, Inc. The siRNA was transfected into glioma cells using the Lipofectamine RNAimax Reagent (Thermo Fisher Scientific) according to the manufacturer's protocol. The negative control siRNA was from Qiagen.

Drugs and drug treatment

TMZ (from Dr. Geoff Margison, The University of Manchester, Manchester, UK) stocks were dissolved in DMSO (Carl Roth GmbH), diluted in two parts sterile dH_2O to a concentration of 35 mmol/L, aliquoted and stored at −80°C until use. CCNU (lomustine; Sigma-Aldrich) was dissolved in absolute ethanol to a stock concentration of 10 mmol/L, aliquoted and stored at −80°C. The MGMT inhibitor O^6-benzylguanine (O^6BG; Sigma-Aldrich) was dissolved in DMSO to a stock concentration of 10 mmol/L, aliquoted and stored at −20°C. One hour before the addition of TMZ or CCNU, MGMT was inhibited by 10 μmol/L O^6BG in order to negate any contribution of MGMT to the cellular responses to these drugs. The p53 inhibitor, pifithrin-α (Sigma-Aldrich) was dissolved in DMSO to a final stock solution of

Published OnlineFirst February 22, 2019; DOI: 10.1158/1541-7786.MCR-18-1306

30 mmol/L, aliquoted and stored at −80 °C. For the inhibition of p53, pifithrin-α (20 μmol/L) was added to the medium 24 hours after TMZ exposure.

Colony survival assay

LN-229, LN-229MGMT and the corresponding HIPK2 knockdown cells were plated onto 6 cm petri dishes at appropriate cell numbers to form at least 100 surviving colonies. Attached cells were exposed to increasing concentrations of TMZ or CCNU, left in the incubator for approximately two weeks, colonies were fixed with acetic acid:methanol:H_2O (1:1:8) and stained with a staining solution (1.25% Giemsa and 0.125% violet crystal). Colonies containing more than 50 cells were scored, colony numbers were adjusted for the cell line's plating efficiency and the surviving fractions were plotted on the graphs.

Apoptosis determination by flow cytometry

For the determination of apoptosis induced by TMZ or CCNU in LN-229, LN-229MGMT, LN-308, LN-229DN-FADD and U87MG, the annexin V/propidium iodide (PI) assay coupled with flow cytometry analysis was used. Following knockdown of either HIPK2, SIAH1, SIAH2 or DcR1, TMZ or CCNU treatment and post-incubation at 37°C, the samples were collected, unfixed cells were labeled with annexin V-FITC (Miltenyi Biotec GmbH) according to the manufacturer's instructions and stained with 1 μg/mL PI (Sigma-Aldrich) before data acquisition by a FACS Canto II flow cytometer (Becton Dickinson GmbH). Annexin V positive cells were classified as apoptotic whereas annexin V and PI double-positive cells were classified as necrotic/late-apoptotic. The data were analyzed using the BD FACSDiva software.

Immunofluorescence microscopy

LN-229 and LN-229 knockdown for HIPK2, for γH2AX and phosphorylated p53 at serine 15 (p-p53ser15) foci, or LN-229, for FAS-L expression, were plated onto glass microscope cover slips. Following exposure to 50 μmol/L TMZ and either 120 hours incubation for γH2AX and p-p53ser15 foci or 72 hours for FAS-L expression, cells were fixed in either ice cold (−20°C) methanol:acetone (7:3) for 9 minutes at −20°C for γH2AX and p-p53ser15 foci or 1% formaldehyde for 30 minutes for FAS-L expression. The first antibodies used were anti-γH2AX (ser139, #9718s) and anti-phospho-p53 (ser15, #9284s) from Cell Signaling Technology and anti-FAS-L (F37720) from Transduction Labs. The second antibodies, coupled to Alexa Fluor 488, were from Invitrogen (Thermo Fisher Scientific). DNA was counterstained with 1 μmol/L TO-PRO-3 (Invitrogen). Slides were mounted in Vectashield antifade mounting medium (Vector Laboratories). Microphotographs were acquired by laser scanning microscopy (LSM710; Carl Zeiss MicroImaging).

Preparation of protein extracts and Western blot analysis

Protein extracts were prepared as previously described (15). Protein concentration was determined by the Bradford method (37). Following separation of proteins by SDS-PAGE and transfer to nitrocellulose membranes, the following antibodies were used: Anti-β-actin, anti-HSP90, anti-p53, anti-FAS, anti-BAX, anti-ERK2, and anti-DcR1, all from Santa Cruz Biotechnology, anti-phospho-p53(S15), anti-phospho-p53(S46), anti-PTEN, anti-PUMA all from Cell Signaling Technology, anti-NOXA and anti-FADD from Calbiochem (Merck/Millipore), anti-MGMT from Chemicon International Inc., and anti-HIPK2, which are privately-produced antibodies already reported on (31). Proteins were detected by the Odyssey 9120 Infrared Imaging System (Li-Cor Biosciences). All Western blots were repeated several times, and representative blots are shown.

Real-time PCR

RNA from cultured LN-229 and LN-229 HIPK2 knockdown cells was isolated using the Direct-zol™ RNA MiniPrep (Zymo Research) Kit. RNA was transcribed into complementary DNA using the Verso cDNA Kit (Thermo Scientific). The PCR was conducted with the SYBR GreenER qPCR SuperMix and a MyIQ Thermal Cycler (Bio-Rad). *HIPK2*-up: 5′-AGGAAGAGTAAGCAGCACCAG-3′, *HIPK2*-low: 5′-TGCTGATGGTGATGACACTGA-3′; *FAS*-up: 5′-TTATCTGATGTTGACTTGAGTAA-3′, *FAS*-low: 5′-GGCTTCATTGACACCATT-3′; *PTEN*-up: 5′-TGCTAACGATCTCTTTGATGATG-3′, *PTEN*-low: 5′-CTACCGCCAAGTCCAGAG-3′; *BBC3*-up: 5′-TTCAGTTTCTCATTGTTAC-3′, *BBC3*-low: 5′-TAAGGATGGAAAGTGTAG-3′; *PMAIP1*-up: 5′-CCAACAGGAACACATTGAAT-3′, *PMAIP1*-low: 5′-TCTTCGGTCACTACACAAC-3′; *BAX*-up: 5′-CAGAAGGCACTAATCAAG-3′, *BAX*-low: 5′-ATCAGATGTGGTCTATAATG-3′; *ACTINB*-up: 5′-GCTACGAGCTGCCTGACG-3′, *ACTINB*-low: 5′-GGCTGGAAGAGTGCCTCA-3′; *GAPDH*-up: 5′-CCCCTCTGGAAAGCTGTGGCGTGAT-3′, *GAPDH*-low: 5′-GGTGGAAGAGTCGGAGTTGCTGTTGA-3′.

Chromatin immune-precipitation and promoter binding experiments

Cells were fixed with 1% formaldehyde for 10 minutes at room temperature and fixation was stopped by adding glycine (125 mmol/L). Cells were lysed in lysis buffer (5 mmol/L PIPES pH 8.0, 85 mmol/L KCl, 0.5% NP40, 1× protease inhibitor) for 10 minutes at 4°C. The nuclei were suspended in ice-cold nuclear lysis buffer (50 mmol/L Tris-HCl pH 8.0, 10 mmol/L EDTA, 0.8% SDS, 1× protease inhibitor) for 10 minutes on ice. The samples were sonicated (20 × 30 seconds), lysates were centrifuged, and the supernatants were collected and precleaned by ChIP-Grade Protein G Magnetic Beads (Cell Signaling Technology; 9006S) in dilution buffer (10 mmol/L Tris-HCl pH 8.0, 0.5 mmol/L EGTA, 140 mmol/L NaCl, 0.1% Na-deoxycholate, 1% triton X-100, 1× protease inhibitor) for 1 hour at 4°C. The precleaned lysates were aliquoted equally and incubated with p-p53ser46 antibody (Becton Dickinson) overnight at 4°C. Saturated protein G magnetic beads were added into each sample and incubated for 2 hours at 4°C. The beads were washed with TSE I (10 mmol/L Tris-HCl pH 8.0, 1 mmol/L EDTA, 0.5 mmol/L EGTA, 140 mmol/L NaCl, 0.1% SDS, 1% triton X-100), TSE II (20 mmol/L Tris-HCl pH 8.0, 2 mmol/L EDTA, 500 mmol/L NaCl, 0.1% SDS, 1% triton X-100), buffer LiCl (10 mmol/L Tris-HCl pH 8.0, 1 mmol/L EDTA, 0.25 M LiCl, 0.5% Na-deoxycholate, 0.5% NP40), and buffer TE (10 mmol/L Tris-HCl pH 8.0, 1 mmol/L EDTA) sequentially. The binding components were eluted in 1% SDS and 0.1 M $NaHCO_3$ and reverse cross-linkage was performed at 65°C overnight. DNA was extracted using the PCR Purification Kit (Qiagen; 28106). Real-time PCR was performed to detect relative enrichment of the protein on indicated genes. The primer used are *FAS-R* -up: 5′-TGAAGCGGAAGTCTGGGAAG-3′, *FAS-R*-low: 5′-GACCTTTGGCTTGGCTTGTC-3′.

Published OnlineFirst February 22, 2019; DOI: 10.1158/1541-7786.MCR-18-1306

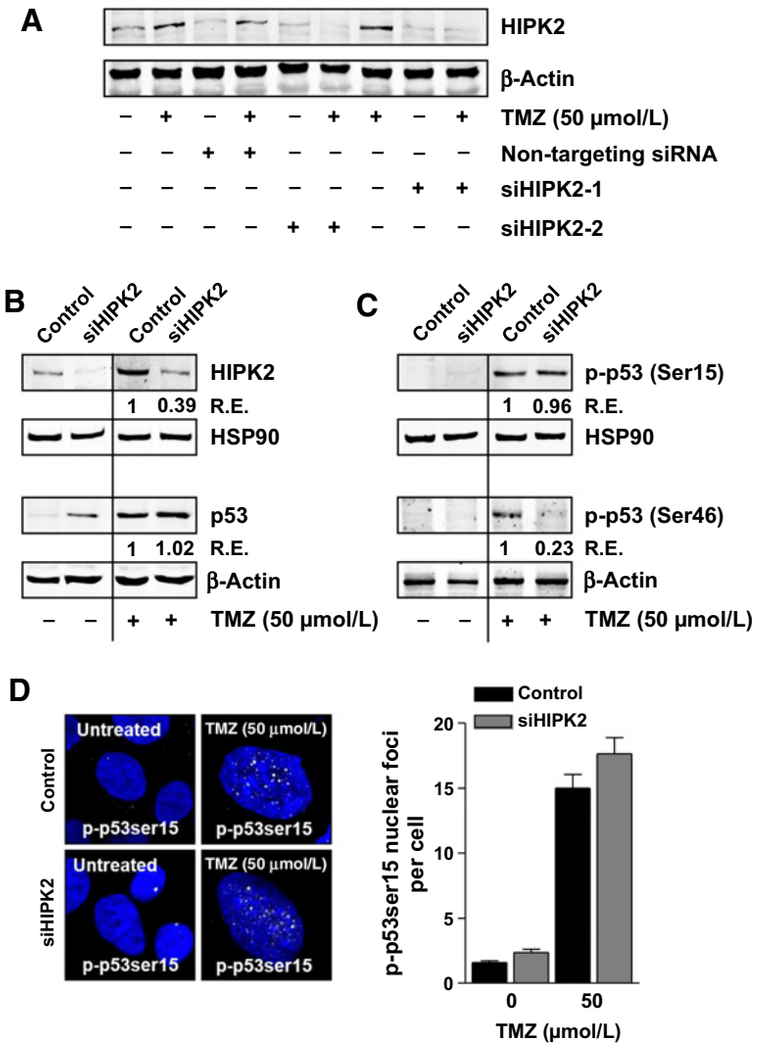

Figure 1.

HIPK2 contributes to the phosphorylation of p53 at serine 46 in glioblastoma cells upon TMZ exposure. **A,** Western blot analysis of siRNA-mediated knockdown of HIPK2 in LN229 cells measured 96 hours after treatment with 50 μmol/L TMZ. Two siRNAs that target different sequences of HIPK2 mRNA was used and nontargeting siRNA was used for control. β-Actin was used as loading control. **B,** Western blot analysis of HIPK2 and total p53 protein. **C,** Western blot analysis of phosphorylated p53 at serine 15 and serine 46 upon HIPK2 knockdown. Cells were harvested 96 hours after 50 μmol/L TMZ. Control samples were transfected with nontargeting siRNA. HSP90 and β-actin were used as loading control. R.E. means relative expression compared to the control. **D,** Left, representative pictures of foci formed by phosphorylated p53ser15 in LN229 cells following 50 μmol/L TMZ exposure and HIPK2 knockdown. Right, quantification of foci formed by phosphorylated p53 at serine 15 in LN229 cells following 50 μmol/L TMZ exposure and HIPK2 knockdown. Data from two independent experiments were collected and up to 360 cells have been counted per measure point and experiment. The difference between untreated and TMZ treated was highly significant ($P < 0.0001$), whereas the difference between non-siRNA and HIPK2-siRNA treated was statistically not significant.

Caspase activity assays

Caspase-3, caspase-8, and caspase-9 activity in LN-229 and LN-229 HIPK2 knockdown cells following TMZ exposure were determined by colourimetric activity assays from Abcam plc, ab39401 for caspase-3, ab39700 for caspase-8, and ab65608 for caspase-9, according to the manufacturer's protocol.

Microarray dataset

A microarray dataset describing the differences in gene expression between samples obtained from 23 patients suffering from epilepsy, 42 patients suffering from grade II oligodendroglioma and astrocytoma, 31 patients suffering from grade III oligodendroglioma and astrocytoma, and 81 patients suffering from grade IV glioblastoma was downloaded from ArrayExpress (https:/www.ebi.ac.uk/arrayexpress). This dataset, namely E-GEOD-4290, was reported on in ref. 38. The intensity values for SIAH1 (NM_003031), SIAH2 (NM_005067), and HIPK2 (NM_022740) were extracted from the dataset and plotted in the graph.

Senescence-associated β-galactosidase staining

Senescence in LN-229 and LN-229 HIPK2 knockdown cells were quantified by senescence-associated β-galactosidase (SA-β-gal) staining according to a previously published protocol (39). Positive blue cells and negative cells were quantified using an Axiover 35 light microscope from Zeiss.

Statistical analysis

For statistical analysis, the unpaired two-tailed *t* test or the one-way ANOVA test was performed using GraphPad Prism version 3 software. *P*-values ≤ 0.05 were considered to be significant and were marked with asterisks in the graphs.

Results

TMZ induces HIPK2, which mediates TMZ-induced phosphorylation of p53 at serine 46

To determine the possible role of HIPK2 in glioblastoma cell death upon TMZ treatment, the conditions for its knockdown had to be established. To this end, LN-229 cells were exposed to TMZ and the amount of HIPK2 was monitored by Western blot analysis. HIPK2 was expressed in LN-229 cells and upon TMZ exposure, the protein level of HIPK2 increased indicating that TMZ induces HIPK2 accumulation (Fig. 1A), presumably through HIPK2 stabilization as described previously for DNA damaging

Published OnlineFirst February 22, 2019; DOI: 10.1158/1541-7786.MCR-18-1306

conditions (27, 31, 40). Using siRNAs that target two different sequences of HIPK2 mRNA (siHIPK2-1 and siHIPK2-2), LN-229 cells were exposed to TMZ following HIPK2 knockdown. Both siHIPK2-1 and siHIPK2-2 abolished the TMZ-induced stabilization of HIPK2 (Fig. 1A). As siHIPK2-2 was more efficient in knocking down HIPK2 upon TMZ exposure, this siRNA was used in the subsequent experiments.

It has been reported that upon exposure of cells to DNA damaging agents such as ultraviolet light, HIPK2 specifically phosphorylates p53 at serine 46 (26). To determine whether this is also the case for the chemotherapeutic TMZ, LN-229 cells were exposed to TMZ in the presence and absence of HIPK2 knockdown. Treatment with TMZ gives rise to p53 stabilization (Fig. 1B) and its phosphorylation at serine 15 and serine 46 (Fig. 1C). Although knockdown of HIPK2 had no effect on the level of p53 stabilization and on TMZ-induced p-p53ser15, HIPK2 depletion strongly reduced the level of p-p53ser46 (Fig. 1B and C). The selective effect of HIPK2 kd on p53ser46 was confirmed by measuring p-p53ser15 foci (41), which were clearly induced by TMZ, but not affected by HIPK2 downregulation (Fig. 1D). These data show that, upon TMZ exposure, HIPK2 plays a role in the phosphorylation of p53 at serine 46, while not affecting the stabilization of p53 nor its phosphorylation at serine 15.

HIPK2 sensitizes glioma cells to the DNA lesion O^6MeG by stimulating the apoptotic response

Next, we determined whether downregulation of HIPK2 has an impact on cell survival. We used LN-229 cells, which lack MGMT, and LN-229 stably transfected with MGMT cDNA (LN-229MGMT; ref. 35; Fig. 2A, insert). As shown by colony-forming experiments, LN-229MGMT cells were completely resistant to TMZ whereas MGMT deficient LN-229 cells died, as expected, in a dose-dependent manner. Knockdown of HIPK2 increased the survival of LN-229 cells following TMZ treatment, compared to the control LN-229 cells (Fig. 2A). The gain of resistance to TMZ following HIPK2 downregulation was confirmed by quantifying the role of HIPK2 in TMZ-induced apoptosis. Upon treatment with 50 μmol/L TMZ, about 40% of LN-229 cells were apoptotic (annexin V positive cells) whereas in the LN-229 HIPK2 knockdown, the level was markedly reduced to 20%. In LN-229MGMT cells, TMZ did not induce apoptosis (Fig. 2B), showing that the effects observed in LN-229 cells, both in the presence and absence of HIPK2, were brought about by the specific DNA lesion O^6MeG. Necrosis (annexin V/PI double-positive cells) was barely induced by TMZ (Fig. 2C), which is in line with previous studies, demonstrating that TMZ induces death in glioblastoma cells mainly through apoptosis (15). TMZ has also been shown to induce, in the same time frame, senescence (34). The induction of senescence by TMZ was quantified by SA-β-Gal and it was shown that senescence was not affected by HIPK2 downregulation (Supplementary Fig. S1). Thus, HIPK2 specifically regulates TMZ-induced apoptosis.

A second line drug in glioblastoma therapy is CCNU, which is a chloroethylating agent forming secondary DNA crosslinks. Although HIPK2 downregulation had a significant impact on TMZ-induced cell death, it neither impacted colony formation (Supplementary Fig. S2A) nor apoptosis (Supplementary Fig. S2B) or necrosis (Supplementary Fig. S2C) following CCNU treatment. As expected, MGMT strongly reduced the killing effect of CCNU (Supplementary Fig. S2B) due to its ability to repair

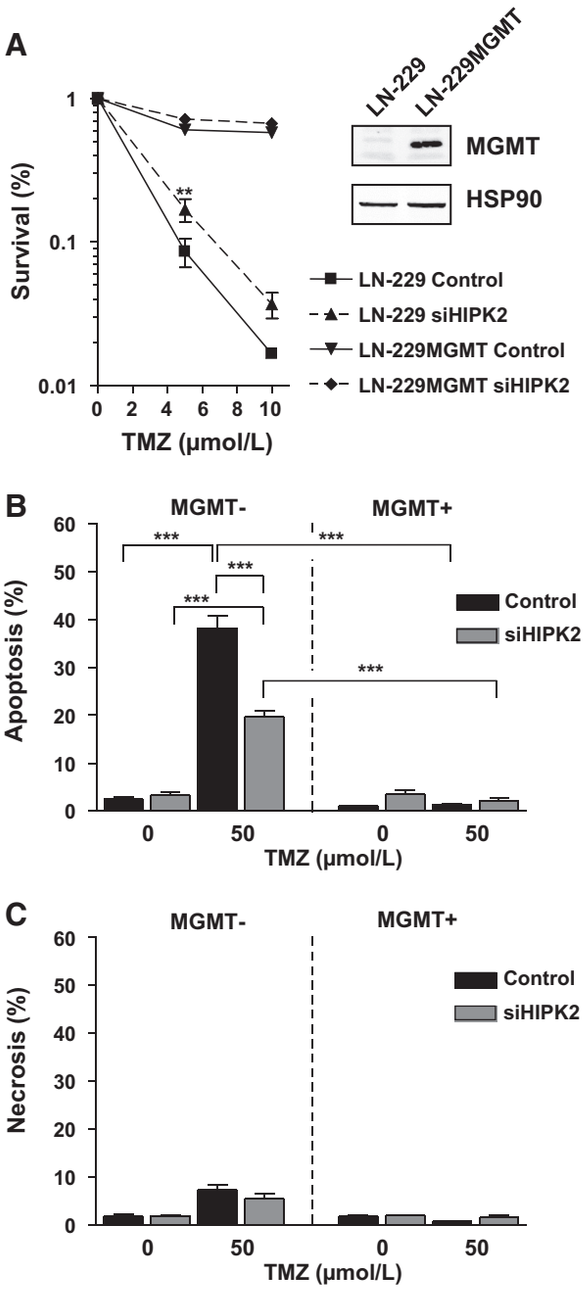

Figure 2.

HIPK2 stimulates apoptosis triggered by the TMZ-induced DNA lesion O^6-MeG in glioblastoma cells. **A,** Colony survival assay of LN229 and LN229 transfected with MGMT (LN229MGMT) exposed to the indicated concentrations of TMZ upon HIPK2 knockdown (left). Western blot analysis of MGMT protein expression in LN229 and LN229MGMT (right). HSP90 was used as loading control. **B,** Apoptosis and (**C**) necrosis induced by TMZ in LN229 and LN229MGMT cells in the control and following HIPK2 knockdown, measured 144 hours after TMZ treatment. Apoptosis is the annexinV positive fraction, necrosis the annexinV/PI positive fraction, % of total population. The control samples were transfected with nontargeting siRNA. Significance levels (*P* values) <0.005 are marked as ** and <0.001 as ***.

Published OnlineFirst February 22, 2019; DOI: 10.1158/1541-7786.MCR-18-1306

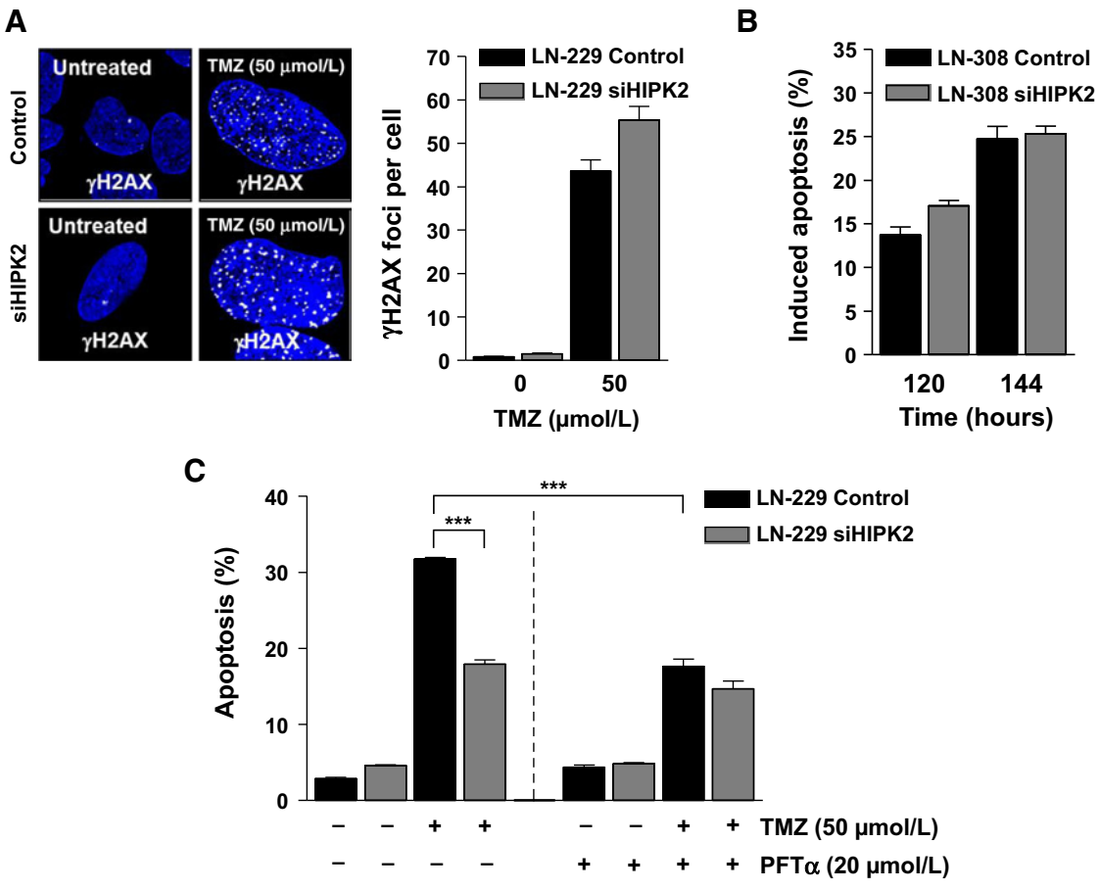

Figure 3.

HIPK2 promotes TMZ-induced apoptosis in a p53-dependent manner, without effecting TMZ-induced DSB formation. **A,** γH2AX foci quantified by fluorescence microscopy in LN229 cells exposed to 50 μmol/L TMZ upon HIPK2 knockdown. Left, representative pictures show TMZ-induced γH2AX foci in white and nuclear staining in blue. Right, quantification of γH2AX foci per cell. Data from two independent experiments were collected and up to 157 cells were counted per measure point and experiment. The difference between untreated and TMZ treatment was highly significant ($P < 0.0001$), whereas the difference between non-siRNA and HIPK2-siRNA treated was statistically not significant. **B,** Apoptosis induced by 50 μmol/L TMZ in LN308 cells upon HIPK2 knockdown. **C,** Inhibition of p53 by pifithrin-α (PFTα) in LN229 cells upon 50 μmol/L TMZ exposure and HIPK2 knockdown. Assay was performed 144 hours after TMZ exposure. *P* values of <0.001 are marked as ***. All control samples were transfected with nontargeting (scrabled) siRNA.

O^6-chloroethylguanine adducts (42). Collectively, the data show that HIPK2 sensitizes glioma cells to the TMZ-induced DNA lesion O^6MeG by stimulating apoptosis.

HIPK2 causes glioblastoma cell sensitization to TMZ-induced apoptosis in a p53-dependent manner

HIPK2 is a kinase that is activated by the DDR, downstream from ATM and ATR (27, 31). To exclude the possibility that the downregulation of HIPK2 has an impact on DNA damage detection and the activation of the DDR, notably in the presence of DSBs, we quantified the extent of γH2AX foci formation. Upon treatment with 50 μmol/L TMZ, LN-229 cells contained an average number of about 40 γH2AX foci, which did not significantly change following HIPK2 knockdown (Fig. 3A). This indicates that HIPK2 has no impact on DSB formation upon TMZ, but works downstream in the DDR.

Because HIPK2 was shown to target p53 (26), its role in TMZ-induced apoptosis was assessed next. If the sensitization to TMZ-induced apoptosis by HIPK2 is dependent on p53, then glioma cells that lack p53 should not differ in their apoptosis response upon HIPK2 knockdown. This was indeed the case, as the p53 null LN-308 cell line did not differ in the TMZ-induced apoptosis response following HIPK2 knockdown compared with the control (Fig. 3B). To substantiate the p53-dependent action of HIPK2 in the sensitization of glioblastoma cells to TMZ, p53 was inhibited with pifithrin-α in LN-229 cells. Inhibition of p53 protected LN-229 cells from TMZ-induced apoptosis (Fig. 3C), showing that p53 stimulates apoptosis induced by TMZ. Simultaneously inhibiting p53 and knocking down HIPK2 had no additional effects on TMZ-induced apoptosis compared with p53 inhibition or HIPK2 knockdown on their own (Fig. 3C). These data support the notion that HIPK2-mediated apoptosis following TMZ in glioblastoma cells is dependent on p53.

HIPK2 stimulates the expression of death receptor FAS upon TMZ exposure

Having shown that HIPK2 sensitizes glioblastoma cells in a p53-dependent manner upon TMZ, we addressed the question

Published OnlineFirst February 22, 2019; DOI: 10.1158/1541-7786.MCR-18-1306

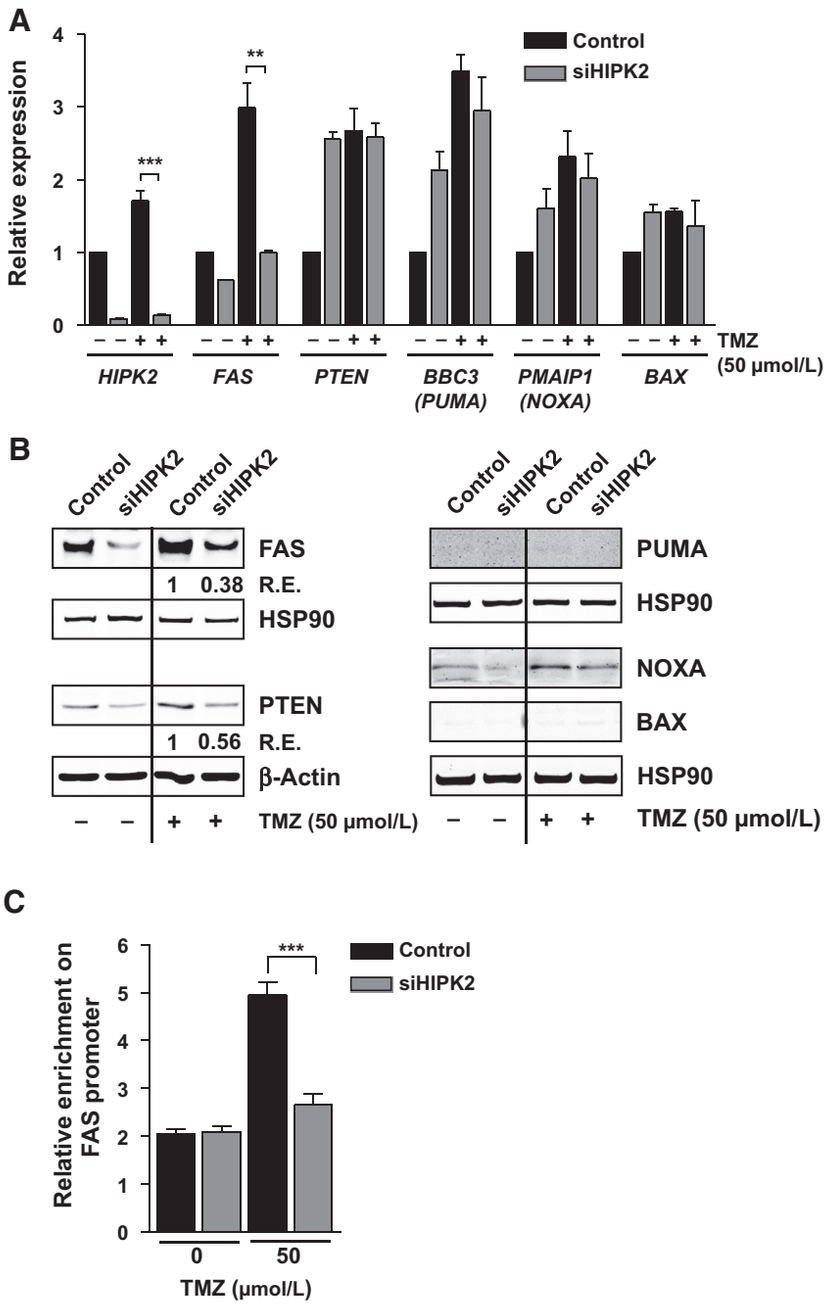

Figure 4.

HIPK2 plays a role in TMZ-induced expression of FAS. **A,** Analysis of *HIPK2, FAS, PTEN, BBC3* (PUMA), *PMAIP1* (NOXA), and *BAX* gene expression by RT-PCR in LN229 cells 72 hours after 50 μmol/L TMZ treatment and HIPK2 knockdown. *P* values of <0.005 are marked as ** and <0.001 as ***. **B,** Western blot analysis of FAS, PTEN, PUMA, NOXA, and BAX protein level in LN229 cells 96 hours after 50 μmol/L TMZ treatment and HIPK2 knockdown. HSP90 and β-actin were used as loading control. R.E. relative expression compared with control. **C,** Binding of p53ser46 on chromatin containing the FAS promoter. Fas promoter DNA following ChIP was determined by quantitative PCR. The outcome is expressed in relation to LN229 control extract precipitated with IgG antibody, which was set to 1. In cells treated with 50 μmol/L TMZ and HIPK2 siRNA significant less p53ser46 was found in the chromatin containing the Fas promoter sequence.

whether HIPK2 activates a specific p53-dependent apoptosis pathway. As shown in Fig. 1B, downregulation of HIPK2 had an impact on TMZ-induced p-p53ser46, which is thought to regulate pro-apoptotic genes. Therefore, we set out to determine the expression level of a set of genes involved in apoptosis. As shown in Fig. 4A, HIPK2 knockdown caused a significant reduction in HIPK2 mRNA (as expected) and, concomitantly, the level of TMZ-induced FAS (alias CD95/APO1) mRNA. For *PTEN*, *BBC3* (PUMA), *PMAIP1* (NOXA), and *BAX*, HIPK2 knockdown had no effect on mRNA level in nontreated and TMZ-treated cells. These results suggest the death receptor FAS as main target of p-p53ser46 that becomes activated by TMZ-induced DNA lesions. This notion was confirmed by Western blot experiments, which showed that FAS is clearly upregulated following treatment with TMZ and this upregulation was abrogated by HIPK2 knockdown (Fig. 4B, left). In addition, there was a slight effect on PTEN expression, whereas the protein levels of PUMA, NOXA, and BAX remained unaffected following TMZ when HIPK2 was downregulated (Fig. 4B). The regulation of *FAS* through HIPK2 via the p53 pathway was further substantiated in chromatin immunoprecipitation (ChIP) experiments. The results showed that following TMZ treatment, binding of p53 to a p53 consensus sequence in the FAS promoter was

Published OnlineFirst February 22, 2019; DOI: 10.1158/1541-7786.MCR-18-1306

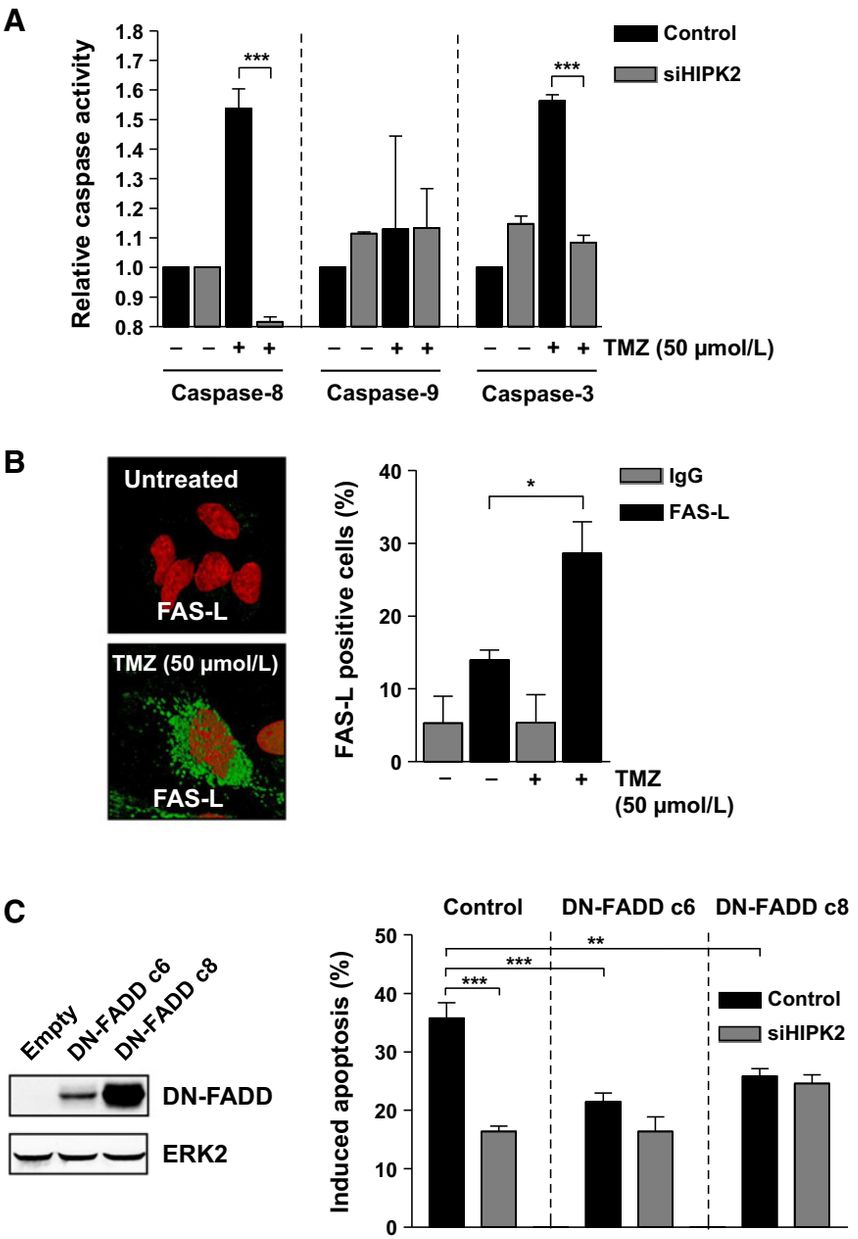

Figure 5.
HIPK2 sensitizes glioblastoma cells to TMZ-induced apoptosis via the activation of the death receptor pathway. **A,** Relative caspase-8, caspase-9, and caspase-3 activity in LN229 cells 96 hours after 50 μmol/L TMZ exposure and HIPK2 knockdown. **B,** Left, representative pictures of cells stained for FAS-L 72 hours after 50 μmol/L TMZ exposure of LN229 cells, as determined by fluorescence microscopy. Right, percentage of FAS-L positive cells 72 hours after 50 μmol/L TMZ exposure in LN229 cells quantified by flow cytometry. **C,** Apoptosis induced by 50 μmol/L TMZ in LN229 cells stably transfected with dominant-negative FADD. Left, Western blot analysis of DN-FADD in LN229 control cells (transfected with the empty vector) and two FADD overexpressing strains, LN229DN-FADDc6 and LN229DN-FADDc8. ERK2 was used as loading control. Right, quantification of apoptosis in the LN229 control and DN-FADD expressing cells DN-FADD c6 and DN-FADD c8 following 50 μmol/L TMZ and HIPK2 knockdown, as measured 144 hours after the begin of TMZ treatment. For (**A**) and (**C**), control samples were transfected with nontargeting siRNA. *P* values of <0.005 are marked as ** and < 0.001 as ***.

substantially enhanced (Fig. 4C). Collectively, these results indicate a critical role for HIPK2 in regulating p53-driven Fas expression in response to TMZ treatment.

HIPK2 stimulates TMZ-induced apoptosis in a death receptor-dependent manner

As HIPK2 knockdown abolished the expression of the p53 target gene *FAS*, the function of this death receptor upon TMZ exposure of glioblastoma cells was examined in more detail. To this end, the influence of HIPK2 knockdown on TMZ triggered caspase activity was determined. Upon exposure of LN-229 cells to TMZ, caspase-8 and caspase-3, but not significantly caspase-9 (for which a high variability was observed), became activated (Fig. 5A), indicating that TMZ triggers the death receptor-dependent apoptosis pathway, which is in line with previous published findings (15). HIPK2 knockdown decreased both the activation of caspase-8 and -3 following TMZ, supporting a role for HIPK2 in the stimulation of TMZ-induced death receptor activation.

Next, the question of whether TMZ is able to induce the expression of FAS ligand (FAS-L) was addressed. Upon exposure of LN-229 cells to TMZ, the cells exhibited a robust increase in FAS-L levels (Fig. 5B). In addition, LN-229 cells were created that are defective in the activation of death receptor downstream signaling. This was accomplished by stably overexpressing a truncated, dominant-negative form of FADD (DN-FADD) in LN-229 cells (Fig. 5C, left). Expression of DN-FADD protected LN-229 cells from TMZ-induced apoptosis (Fig. 5C, right), further supporting the role of the death receptor in TMZ-induced

Published OnlineFirst February 22, 2019; DOI: 10.1158/1541-7786.MCR-18-1306

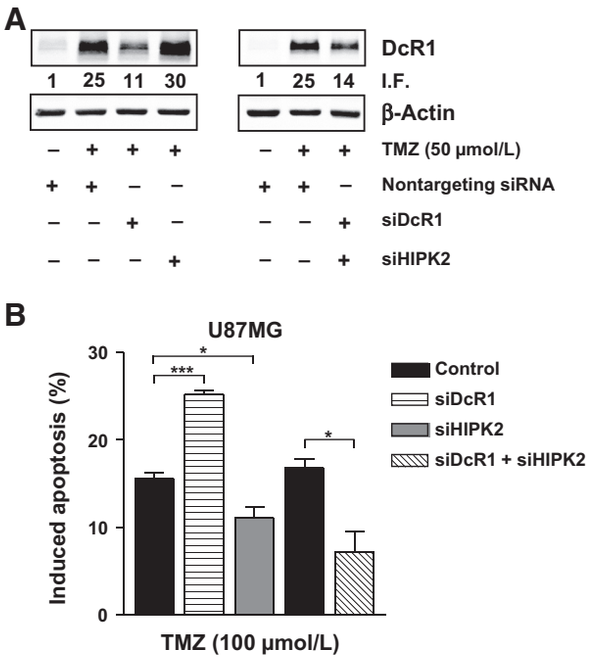

Figure 6.

Role of DcR1 in the HIPK2-mediated killing response. **A,** Western blot analysis of DcR1 protein levels after 50 μmol/L TMZ exposure, DcR1, HIPK2, and DcR1 and HIPK2 knockdown in U87MG cells. I.F. induction factor. β-Actin was used as loading control. **B,** Induction of apoptosis in U87MG cells after 50 μmol/L TMZ exposure, DcR1, HIPK2, and DcR1 and HIPK2 knockdown. Control samples were transfected with nontargeting siRNA.

apoptosis. Knockdown of HIPK2 had no influence on apoptosis in the DN-FADD expressing cells, showing that HIPK2 is unable to sensitize glioblastoma cells if death receptor signaling is nonfunctional.

The p53-dependent activation of the death receptor by TMZ (15) was shown to be counteracted by simultaneous NF-κB–dependent activation of the decoy receptor DcR1 (43). Theoretically, DcR1 knockdown should sensitize glioma cells to TMZ-induced apoptosis whereas simultaneous knockdown of DcR1 and HIPK2 should still lead to resistance. This was, in fact, the case as knockdown of DcR1 in U87MG glioma cells (shown in Fig. 6A) leads to sensitization, knockdown of HIPK2 to resistance and simultaneous knockdown of DcR1 and HIPK2 still resulted in resistance, i.e. significantly lowering the TMZ-induced apoptosis frequency (Fig. 6B). Of note, U87MG showed the same phenotype following HIPK2 knockdown and TMZ treatment as LN-229 cells, supporting the role of HIPK2 in wild-type p53-expressing glioma cells. Collectively, the data lend support for HIPK2 stimulating apoptosis by targeting p53 to the promoter of FAS in TMZ-treated cells.

The role of SIAH1 in HIPK2 activation in glioblastoma cells following TMZ treatment

Key player in the regulation of HIPK2 stabilization is the E3 ubiquitin-protein ligase SIAH1 (31). For UV light it has been shown that following phosphorylation by ATM/ATR, SIAH1 is released from HIPK2 and HIPK2 protein accumulates. For SIAH2 similar data are not available. In view of this scenario, the influence of SIAH1 on TMZ-induced apoptosis was determined by downregulation of SIAH1, SIAH2, or both. As shown in Fig. 7A, TMZ treatment gave rise to HIPK2 stabilization, which was enhanced upon SIAH1 (siSIAH1) or SIAH1 together with SIAH2 (siSIAH1&2) knockdown, but not when only SIAH2 (siSIAH2) was downregulated. Accordingly, TMZ-induced apoptosis was significantly enhanced when SIAH1 or SIAH1&SIAH 2 were knocked down (Fig. 7B). Sensitization was not observed for SIAH2 knockdown (Fig. 7B). The data support the notion that SIAH1, but not SIAH2, plays a critical role in cell death regulation in TMZ-treated glioblastoma cells.

Overall, the data provide compelling evidence that HIPK2 and its inhibitor, SIAH1, are involved in the complex scenario regulating the sensitivity of glioblastoma cells to TMZ. This leads to the question of how HIPK2 and SIAH1/2 are expressed in gliomas. An *in silico* search for expression levels revealed that HIPK2 is expressed in glioblastoma multiforme *in situ* at about the same level as in normal brain and low-grade gliomas. The same is true for SIAH2. In contrast, SIAH1 is frequently overexpressed in gliomas, notably in glioblastoma multiforme (Fig. 7C). In view of the inhibitor function of SIAH1 on HIPK2, the data bear significant implications as tumors with high SIAH1 are predicted to have a low response on TMZ treatment.

Discussion

This work was aimed at assessing the role of HIPK2 (25, 26) and its negative regulating E3 ubiquitin ligases SIAH1 and SIAH2 (31, 44) in the regulation of apoptosis triggered by the specific alkylation damage O^6MeG. This DNA adduct is induced by methylating anticancer drugs such as TMZ, which is the first-line therapeutic for the treatment of high-grade malignant gliomas. Like other S_N1 methylating agents (including dacarbazine, procarbazine streptozotozine, and a plethora of environmental and endogenous carcinogens), TMZ induces a broad spectrum of DNA lesions that can be grouped in *O*- and *N*-alkylations. Although produced in small amounts (~5% of total alkylation products), O^6MeG is responsible for the majority of killing effects if TMZ is administered at low dose, that is <100 μmol/L, which is relevant in the therapeutic setting (3).

TMZ at dose levels below 100 μmol/L (here we used maximally 50 μmol/L) induces in glioblastoma cells mainly apoptosis, barely necrosis. The pathway of O^6MeG triggered apoptosis has been elucidated in detail (15). It can be split up into three sections, an upstream genotoxic, a signaling and a downstream execution pathway. Upstream is characterized by the transformation of O^6MeG lesions into DSBs. It is generally accepted that this requires DNA replication and MMR operating on O^6MeG/T mismatches (45). It was shown that MMR generates, following removal of thymine on O^6MeG/T mismatches, long stretches of single-stranded DNA (46), which strongly interfere with DNA replication in the second replication cycle giving rise to transient and, if not properly repaired, persistent DSBs (47). The block in replication, resulting from futile MMR cycles, and DSBs resulting from the collapse of replication forks, are key activators of the downstream DDR pathway evoked by the primary lesion O^6MeG (48, 49).

In the O^6MeG triggered DDR following TMZ treatment, ATR and CHK1 activation plays a key role, followed later on by ATM/CHK2 activation, which is likely a secondary event triggered by non-repaired DSBs at replication forks (33). Both ATR and ATM

Published OnlineFirst February 22, 2019; DOI: 10.1158/1541-7786.MCR-18-1306

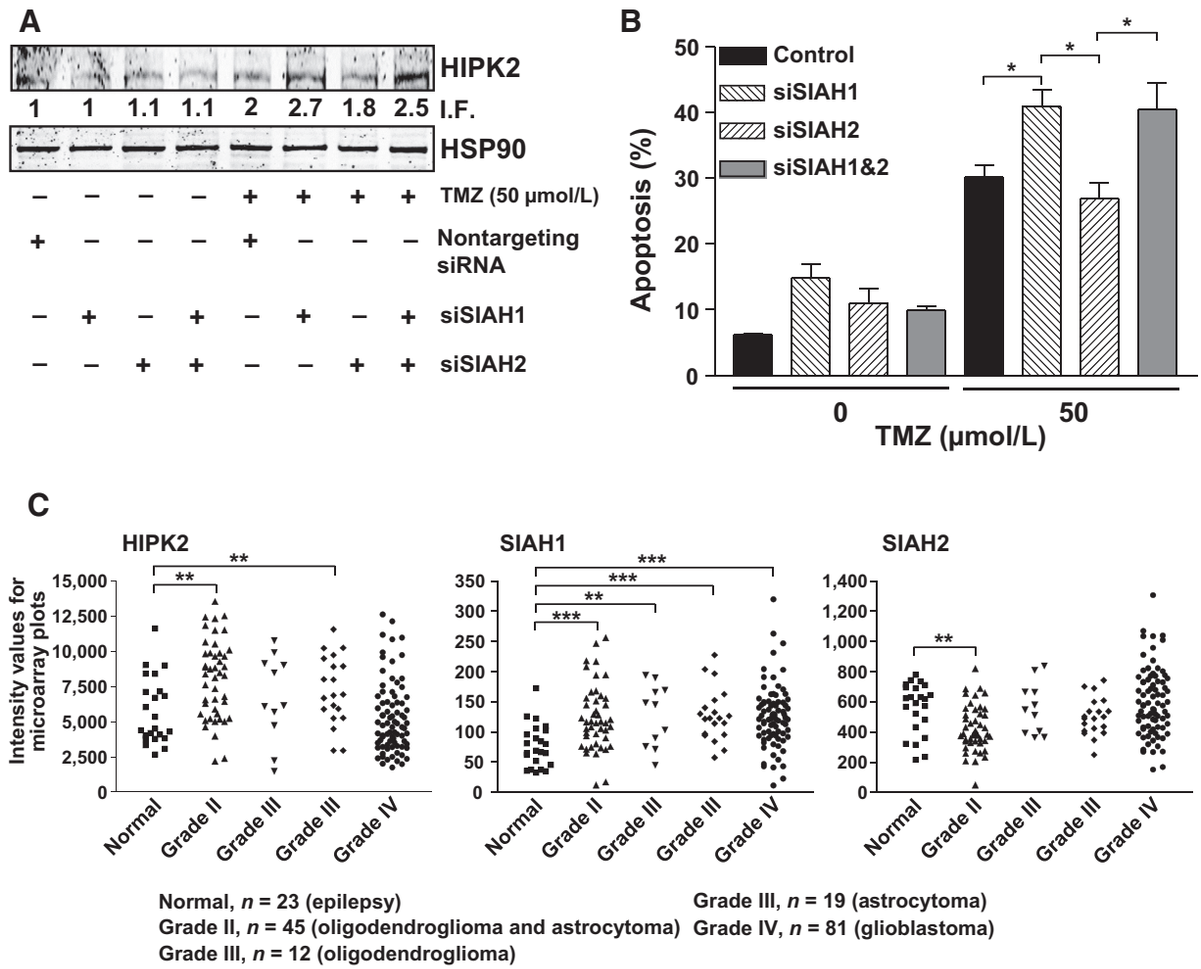

Figure 7.

Impact of SIAH1 on HIPK2 in TMZ-induced apoptosis and expression of SIAH and HIPK2 in human gliomas. **A,** Western blot analysis of HIPK2 in LN229 cells 72 hours after 50 μmol/L TMZ exposure, knocked-down for SIAH1, SIAH2, or SIAH1 and SIAH2. HSP90 was used as loading control. I.F. relative expression compared with nontargeting siRNA only. **B,** Apoptosis levels 144 hours after 50 μmol/L TMZ exposure of LN229 cells knocked-down for SIAH1, SIAH2, or SIAH1 and SIAH2. **C,** Using a public available microarray database, the expression of HIPK2 (NM_022740), SIAH1 (NM_003031), and SIAH2 (NM_005067) was analyzed in brain tissue from 23 epilepsy patients as well as tumor tissue from 45 grade II oligodendroglioma and astrocytoma patients, 12 grade III oligodendroglioma patients, 19 grade III astrocytoma, and 81 glioblastoma (grade IV) patients. *P* values <0.05 are marked as *, <0.005 as **, and <0.001 as ***.

phosphorylate p53 at serine 15, leading to its stabilization (20, 50) and transcriptional activation of target genes such as p21 (22). The protective effect of the p53-dependent cell-cycle arrest observed in glioma cells exposed to TMZ (17) can therefore be traced back to the activation of ATR and ATM (33). Parallel to this protective effect, p53 was identified as transcriptional activator of the death receptor FAS (alias CD95/APO1; ref. 51), which stimulates DNA damage-triggered apoptosis (15). This may explain the finding that p53wt glioblastoma cells are more sensitive to TMZ, responding with a higher yield of apoptosis compared with glioblastoma cells mutated for p53, which utilize the less effective mitochondrial pathway (15). Of note, we observed that downregulation of HIPK2 had no significant impact on the level of γH2AX foci following TMZ treatment, supporting the notion that the proapoptotic effect of HIPK2 is mediated by TMZ-activated downstream functions.

In view of the dichotomic character of p53, we wished to know in more detail how p53 is able to make the decision between survival and death. Unlike p53ser15 (and p53ser20 resulting from CHK1 and CHK2 activation), the phosphorylation of p53 at ser46 is solely mediated by the kinase HIPK2 (26). This DDR enzyme is localized in the nucleus (52) and, under normal conditions (i.e., without genotoxic stress), inactivated by the E3 ubiquitin-protein ligase SIAH1 (32). Upon DNA damage, SIAH1 becomes phosphorylated by ATM or ATR, which results in its dissociation from HIPK2 and, therefore, HIPK2 accumulates in the nucleus (31). HIPK2 in turn phosphorylates p53 at ser46, thus stimulating its transactivating activity. This was shown to be the case for cells exposed to ultraviolet light (25, 26), ionizing radiation (27), cisplatin (29), and the topoisomerase inhibitor doxorubicin (53). Here, we demonstrate for the first time that the S_N1

methylating agent TMZ is able to trigger this pathway. Following TMZ treatment, the level of HIPK2 was found to be enhanced. Importantly, this was attenuated in the presence of ATM inhibitor and completely abrogated upon posttreatment with an ATR inhibitor (Supplementary Fig. S3), which is in line with the notion that ATR/ATM are the upstream kinases triggering this response. It also supports our previous finding that TMZ activates preferentially the ATR–CHK1 pathway (33). Furthermore we were able to identify the critical DNA damage triggering this response, O^6MeG, as MGMT expressing isogenic cells, in which O^6MeG is repaired, do not show HIPK2 activation and p53ser46 phosphorylation. They also do not show HIPK2 stabilization (Supplementary Fig. S3). Obviously, O^6MeG is a highly effective inducer of the ATR/ATM–SIAH1–HIPK2 pathway, which is remarkable as TMZ, like other S_N1 methylating agents, induces at least 12 different DNA lesions, with the minor lesion O^6MeG being so effective in evoking the DDR and killing cells (48). We should note that the major *N*-alkylation lesions also bear cytotoxic potential, but this is only the case if O^6MeG is completely removed by MGMT and a sufficient amount of *N*-alkylations were induced that are not fully repaired by base excision repair. In this case, cells need to be treated with much higher doses of TMZ than used in this study.

We also demonstrate that upon TMZ treatment, HIPK2 is the only kinase phosphorylating p53 at serine 46 since HIPK2 knockdown completely abrogated this response. p-p53ser46 was previously demonstrated to transcriptionally activate several pro-apoptotic target genes, including *PTEN* (24) and *NOXA* (54). However, we did not find an effect of HIPK2 knockdown on the upregulation of these genes, nor on *BBC3* (PUMA) and *BAX* in TMZ-treated p53wt glioblastoma cells. Another transcriptional target of p53 is the death receptor FAS (55, 56), which has been shown to be induced by TMZ in a p53-dependent manner (15). The expression of FAS mRNA and protein was enhanced following O^6MeG induction and reduced if HIPK2 was knocked down. At the same time, the TMZ-induced level of apoptosis was significantly reduced, suggesting that the HIPK2/p-p53ser46/FAS pathway is decisively involved in TMZ-induced apoptosis. This was further substantiated by blocking the FAS pathway through DN-FADD expression, which abrogated the HIPK2-driven apoptotic response. Under the treatment conditions (dose range up to 50 μmol/L TMZ) necrosis was only marginally induced, which indicates that O^6MeG triggered apoptosis plays a major role in cell death induction. Of note, in p53wt glioblastoma cells lower doses of TMZ were required than in p53mt cells for inducing a given apoptosis level, because p53mt cells utilize the less effective mitochondrial pathway (15). We should also note that TMZ-induced senescence, which requires ATR/ATM activation (57), was not impaired by HIPK2 knockdown indicating HIPK2 is not involved in the activation of the TMZ-induced senescence pathway.

Downregulation of either SIAH1, SIAH2, or both SIAH1&2 revealed that SIAH1, but not SIAH2, is the principle regulator of HIPK2 in glioma cells exposed to TMZ. It is striking that gliomas frequently overexpress SIAH1, as revealed by our *in silico* analysis. Therefore, it is conceivable that the fraction of tumors exhibiting a high SIAH1 level is impaired in activating the apoptotic death pathway. Based on these findings, it is reasonable to hypothesize that downregulation, or pharmacologic inhibition, of SIAH1 has a positive impact on therapy with TMZ.

It is important to note that modulation of the HIPK2 pathway had no significant impact on the killing response of glioma cells to CCNU, which is sometimes used concomitantly with TMZ or as second-line therapeutic. CCNU induces O^6-chloroethylguanine and secondary interstrand crosslinks (ICL), which are highly cytotoxic lesions through blocking transcription and replication (42). It thus appears that ICL do not trigger the HIPK2 pathway as efficiently as O^6MeG/MMR-derived lesions do.

In summary, our data revealed a new DDR pathway triggered by the cytotoxic (and mutagenic) DNA lesion O^6MeG. Taking into account previously published data (33, 47), we propose that secondary lesions resulting from the processing of O^6MeG trigger the activation of ATR and, as a secondary event ATM, which phosphorylate SIAH1. This results in HIPK2 stabilization and its kinase activation, p53ser46 phosphorylation, and stimulation of the apoptotic FAS pathway. These findings bear therapeutic implications, paving the way for new strategies in fostering death functions and blocking survival traits in tumor cells. This concept can clearly be extended to other methylating anticancer drugs such as dacarbazine (DTIC), procarbazine, and streptozotocin, which act on molecular level in the same way as TMZ and are being used in the therapy of other cancers such as malignant melanoma, Hodgkin lymphoma, and islet-cell carcinoma (7, 49). Moreover, O^6MeG is not only an important clinically relevant DNA damage as it can also be produced by methylating environmental and food-borne carcinogens such as *N*-nitrosodimethylamine, for which it is considered to be a critical mutagenic and carcinogenic lesion (49, 58). Therefore, the identification of the SIAH1/HIPK2/p53ser46 axis triggered by O^6MeG is not only important for cancer therapy. It also has far-reaching implications for cancer prevention because cells harboring mutagenic and carcinogenic O^6MeG lesions may selectively be removed through this death pathway.

Disclosure of Potential Conflicts of Interest

No potential conflicts of interest were disclosed.

Authors' Contributions

Conception and design: Y. He, T.G. Hofmann, B. Kaina
Development of methodology: Y. He, W.P. Roos, B. Kaina
Acquisition of data (provided animals, acquired and managed patients, provided facilities, etc.): Y. He, W.P. Roos, Q. Wu, B. Kaina
Analysis and interpretation of data (e.g., statistical analysis, biostatistics, computational analysis): Y. He, W.P. Roos, Q. Wu, T.G. Hofmann, B. Kaina
Writing, review, and/or revision of the manuscript: Y. He, W.P. Roos, T.G. Hofmann, B. Kaina
Administrative, technical, or material support (i.e., reporting or organizing data, constructing databases): Y. He, Q. Wu, T.G. Hofmann, B. Kaina
Study supervision: B. Kaina

Acknowledgments

Y. He was a grant holder of the international PhD program on Gene Regulation, Epigenetics and Genome Stability, Mainz, Germany. The work was further supported by grants to B. Kaina from the Deutsche Forschungsgemeinschaft (KA724) and German Cancer Aid. We thank G. Nagel for assistance in the β-gal staining experiments.

The costs of publication of this article were defrayed in part by the payment of page charges. This article must therefore be hereby marked *advertisement* in accordance with 18 U.S.C. Section 1734 solely to indicate this fact.

Received December 6, 2018; revised February 2, 2019; accepted February 18, 2019; published first February 22, 2019.

References

1. Johnson DR, O'Neill BP. Glioblastoma survival in the United States before and during the temozolomide era. J Neurooncol 2012;107:359–64.
2. Stupp R, Mason WP, van den Bent MJ, Weller M, Fisher B, Taphoorn MJ, et al. Radiotherapy plus concomitant and adjuvant temozolomide for glioblastoma. N Engl J Med 2005;352:987–96.
3. Newlands ES, Stevens MF, Wedge SR, Wheelhouse RT, Brock C. Temozolomide: a review of its discovery, chemical properties, pre-clinical development and clinical trials. Cancer Treat Rev 1997;23:35–61.
4. Tisdale MJ. Antitumor imidazotetrazines–XV. Role of guanine O6 alkylation in the mechanism of cytotoxicity of imidazotetrazinones. Biochem Pharmacol 1987;36:457–62.
5. Baer JC, Freeman AA, Newlands ES, Watson AJ, Rafferty JA, Margison GP. Depletion of O6-alkylguanine-DNA alkyltransferase correlates with potentiation of temozolomide and CCNU toxicity in human tumour cells. Br J Cancer 1993;67:1299–302.
6. Christmann M, Nagel G, Horn S, Krahn U, Wiewrodt D, Sommer C, et al. MGMT activity, promoter methylation and immunohistochemistry of pretreatment and recurrent malignant gliomas: a comparative study on astrocytoma and glioblastoma. Int J Cancer 2010;127:2106–18.
7. Kaina B, Christmann M, Naumann S, Roos WP. MGMT: key node in the battle against genotoxicity, carcinogenicity and apoptosis induced by alkylating agents. DNA Repair (Amst) 2007;6:1079–99.
8. Wiewrodt D, Nagel G, Dreimuller N, Hundsberger T, Perneczky A, Kaina B. MGMT in primary and recurrent human glioblastomas after radiation and chemotherapy and comparison with p53 status and clinical outcome. Int J Cancer 2008;122:1391–9.
9. Esteller M, Hamilton SR, Burger PC, Baylin SB, Herman JG. Inactivation of the DNA repair gene O6-methylguanine-DNA methyltransferase by promoter hypermethylation is a common event in primary human neoplasia. Cancer Res 1999;59:793–7.
10. Hegi ME, Diserens AC, Gorlia T, Hamou MF, de Tribolet N, Weller M, et al. MGMT gene silencing and benefit from temozolomide in glioblastoma. N Engl J Med 2005;352:997–1003.
11. Esteller M, Garcia-Foncillas J, Andion E, Goodman SN, Hidalgo OF, Vanaclocha V, et al. Inactivation of the DNA-repair gene MGMT and the clinical response of gliomas to alkylating agents. N Engl J Med 2000;343:1350–4.
12. Roos W, Baumgartner M, Kaina B. Apoptosis triggered by DNA damage O6-methylguanine in human lymphocytes requires DNA replication and is mediated by p53 and Fas/CD95/Apo-1. Oncogene 2004;23:359–67.
13. Happold C, Roth P, Wick W, Schmidt N, Florea AM, Silginer M, et al. Distinct molecular mechanisms of acquired resistance to temozolomide in glioblastoma cells. J Neurochem 2012;122:444–55.
14. Ochs K, Kaina B. Apoptosis induced by DNA damage O6-methylguanine is Bcl-2 and caspase-9/3 regulated and Fas/caspase-8 independent. Cancer Res 2000;60:5815–24.
15. Roos WP, Batista LF, Naumann SC, Wick W, Weller M, Menck CF, et al. Apoptosis in malignant glioma cells triggered by the temozolomide-induced DNA lesion O6-methylguanine. Oncogene 2007;26:186–97.
16. Hermisson M, Klumpp A, Wick W, Wischhusen J, Nagel G, Roos W, et al. O6-methylguanine DNA methyltransferase and p53 status predict temozolomide sensitivity in human malignant glioma cells. J Neurochem 2006;96:766–76.
17. Hirose Y, Berger MS, Pieper RO. p53 effects both the duration of G_2–M arrest and the fate of temozolomide-treated human glioblastoma cells. Cancer Res 2001;61:1957–63.
18. Fulci G, Ishii N, Van Meir EG. p53 and brain tumors: from gene mutations to gene therapy. Brain Pathol 1998;8:599–613.
19. Roos WP, Thomas AD, Kaina B. DNA damage and the balance between survival and death in cancer biology. Nat Rev Cancer 2016;16:20–33.
20. Nakagawa K, Taya Y, Tamai K, Yamaizumi M. Requirement of ATM in phosphorylation of the human p53 protein at serine 15 following DNA double-strand breaks. Mol Cell Biol 1999;19:2828–34.
21. Bode AM, Dong Z. Post-translational modification of p53 in tumorigenesis. Nat Rev Cancer 2004;4:793–805.
22. Loughery J, Cox M, Smith LM, Meek DW. Critical role for p53-serine 15 phosphorylation in stimulating transactivation at p53-responsive promoters. Nucleic Acids Res 2014;42:7666–80.
23. Oda K, Arakawa H, Tanaka T, Matsuda K, Tanikawa C, Mori T, et al. p53AIP1, a potential mediator of p53-dependent apoptosis, and its regulation by Ser-46-phosphorylated p53. Cell 2000;102:849–62.
24. Mayo LD, Seo YR, Jackson MW, Smith ML, Rivera Guzman J, Korgaonkar CK, et al. Phosphorylation of human p53 at serine 46 determines promoter selection and whether apoptosis is attenuated or amplified. J Biol Chem 2005;280:25953–9.
25. Hofmann TG, Moller A, Sirma H, Zentgraf H, Taya Y, Droge W, et al. Regulation of p53 activity by its interaction with homeodomain-interacting protein kinase-2. Nat Cell Biol 2002;4:1–10.
26. D'Orazi G, Cecchinelli B, Bruno T, Manni I, Higashimoto Y, Saito S, et al. Homeodomain-interacting protein kinase-2 phosphorylates p53 at Ser 46 and mediates apoptosis. Nat Cell Biol 2002;4:11–9.
27. Dauth I, Kruger J, Hofmann TG. Homeodomain-interacting protein kinase 2 is the ionizing radiation-activated p53 serine 46 kinase and is regulated by ATM. Cancer Res 2007;67:2274–9.
28. Bitomsky N, Conrad E, Moritz C, Polonio-Vallon T, Sombroek D, Schultheiss K, et al. Autophosphorylation and Pin1 binding coordinate DNA damage-induced HIPK2 activation and cell death. Proc Natl Acad Sci U S A 2013;110:E4203–12.
29. Di Stefano V, Blandino G, Sacchi A, Soddu S, D'Orazi G. HIPK2 neutralizes MDM2 inhibition rescuing p53 transcriptional activity and apoptotic function. Oncogene 2004;23:5185–92.
30. Kodama M, Otsubo C, Hirota T, Yokota J, Enari M, Taya Y. Requirement of ATM for rapid p53 phosphorylation at Ser46 without Ser/Thr-Gln sequences. Mol Cell Biol 2010;30:1620–33.
31. Winter M, Sombroek D, Dauth I, Moehlenbrink J, Scheuermann K, Crone J, et al. Control of HIPK2 stability by ubiquitin ligase Siah-1 and checkpoint kinases ATM and ATR. Nat Cell Biol 2008;10:812–24.
32. Matt S, Hofmann TG. The DNA damage-induced cell death response: a roadmap to kill cancer cells. Cell Mol Life Sci 2016;73:2829–50.
33. Eich M, Roos WP, Nikolova T, Kaina B. Contribution of ATM and ATR to the resistance of glioblastoma and malignant melanoma cells to the methylating anticancer drug temozolomide. Mol Cancer Ther 2013;12:2529–40.
34. Knizhnik AV, Roos WP, Nikolova T, Quiros S, Tomaszowski KH, Christmann M, et al. Survival and death strategies in glioma cells: autophagy, senescence and apoptosis triggered by a single type of temozolomide-induced DNA damage. PLoS One 2013;8:e55665.
35. Quiros S, Roos WP, Kaina B. Rad51 and BRCA2–New molecular targets for sensitizing glioma cells to alkylating anticancer drugs. PLoS One 2011;6:e27183.
36. Tewari M, Dixit VM. Fas- and tumor necrosis factor-induced apoptosis is inhibited by the poxvirus crmA gene product. J Biol Chem 1995;270:3255–60.
37. Bradford MM. A rapid and sensitive method for the quantitation of microgram quantities of protein utilizing the principle of protein-dye binding. Anal Biochem 1976;72:248–54.
38. Sun L, Hui AM, Su Q, Vortmeyer A, Kotliarov Y, Pastorino S, et al. Neuronal and glioma-derived stem cell factor induces angiogenesis within the brain. Cancer Cell 2006;9:287–300.
39. Debacq-Chainiaux F, Erusalimsky JD, Campisi J, Toussaint O. Protocols to detect senescence-associated beta-galactosidase (SA-betagal) activity, a biomarker of senescent cells in culture and in vivo. Nat Protoc 2009;4:1798–806.
40. Crone J, Glas C, Schultheiss K, Moehlenbrink J, Krieghoff-Henning E, Hofmann TG. Zyxin is a critical regulator of the apoptotic HIPK2-p53 signaling axis. Cancer Res 2011;71:2350–9.
41. Hampp S, Kiessling T, Buechle K, Mansilla SF, Thomale J, Rall M, et al. DNA damage tolerance pathway involving DNA polymerase iota and the tumor suppressor p53 regulates DNA replication fork progression. Proc Natl Acad Sci U S A 2016;113:E4311–9.
42. Nikolova T, Roos WP, Kramer OH, Strik HM, Kaina B. Chloroethylating nitrosoureas in cancer therapy: DNA damage, repair and cell death signaling. Biochim Biophys Acta 2017;1868:29–39.
43. Mansour NM, Bernal GM, Wu L, Crawley CD, Cahill KE, Voce DJ, et al. Decoy receptor DcR1 is induced in a p50/Bcl3-dependent manner and attenuates the efficacy of temozolomide. Cancer Res 2015;75:2039–48.
44. Calzado MA, de la Vega L, Moller A, Bowtell DD, Schmitz ML. An inducible autoregulatory loop between HIPK2 and Siah2 at the apex of the hypoxic response. Nat Cell Biol 2009;11:85–91.

45. Kaina B, Ziouta A, Ochs K, Coquerelle T. Chromosomal instability, reproductive cell death and apoptosis induced by O6-methylguanine in Mex-, Mex+ and methylation-tolerant mismatch repair compromised cells: facts and models. Mutation Res 1997;381:227–41.
46. Mojas N, Lopes M, Jiricny J. Mismatch repair-dependent processing of methylation damage gives rise to persistent single-stranded gaps in newly replicated DNA. Genes Dev 2007;21:3342–55.
47. Quiros S, Roos WP, Kaina B. Processing of O6-methylguanine into DNA double-strand breaks requires two rounds of replication whereas apoptosis is also induced in subsequent cell cycles. Cell Cycle 2010;9:168–78.
48. Roos WP, Kaina B. DNA damage-induced cell death: from specific DNA lesions to the DNA damage response and apoptosis. Cancer Lett 2013;332:237–48.
49. Fu D, Calvo JA, Samson LD. Balancing repair and tolerance of DNA damage caused by alkylating agents. Nat Rev Cancer 2012;12:104–20.
50. Hammond EM, Denko NC, Dorie MJ, Abraham RT, Giaccia AJ. Hypoxia links ATR and p53 through replication arrest. Mol Cell Biol 2002;22:1834–43.
51. Muller M, Wilder S, Bannasch D, Israeli D, Lehlbach K, Li-Weber M, et al. p53 activates the CD95 (Apo-1/Fas) gene in response to DNA damage by anticancer drugs. J Exp Med 1998;188:2033–45.
52. Siepi F, Gatti V, Camerini S, Crescenzi M, Soddu S. HIPK2 catalytic activity and subcellular localization are regulated by activation-loop Y354 autophosphorylation. Biochim Biophys Acta 2013;1833:1443–53.
53. Puca R, Nardinocchi L, Sacchi A, Rechavi G, Givol D, D'Orazi G. HIPK2 modulates p53 activity towards pro-apoptotic transcription. Mol Cancer 2009;8:85.
54. Ichwan SJ, Yamada S, Sumrejkanchanakij P, Ibrahim-Auerkari E, Eto K, Ikeda MA. Defect in serine 46 phosphorylation of p53 contributes to acquisition of p53 resistance in oral squamous cell carcinoma cells. Oncogene 2006;25:1216–24.
55. Muller M, Wilder S, Bannasch D, Israeli D, Lehlbach K, Li-Weber M, et al. p53 activates the CD95 (APO-1/Fas) gene in response to DNA damage by anticancer drugs. J Exp Med 1998;188:2033–45.
56. Pohl U, Wagenknecht B, Naumann U, Weller M. p53 enhances BAK and CD95 expression in human malignant glioma cells but does not enhance CD95L-induced apoptosis. Cell Physiol Biochem 1999;9:29–37.
57. Aasland D, Gotzinger L, Hauck L, Berte N, Meyer J, Effenberger M, et al. Temozolomide induces senescence and repression of DNA repair pathways in glioblastoma cells via activation of ATR-CHK1, p21, and NF-kappaB. Cancer Res 2019;79:99–113.
58. Lijinsky W. N-Nitroso compounds in the diet. Mutat Res 1999;443:129–38.

Published OnlineFirst February 22, 2019; DOI: 10.1158/1541-7786.MCR-18-1306

Molecular Cancer Research

The SIAH1–HIPK2–p53ser46 Damage Response Pathway is Involved in Temozolomide-Induced Glioblastoma Cell Death

Yang He, Wynand P. Roos, Qianchao Wu, et al.

Mol Cancer Res 2019;17:1129-1141. Published OnlineFirst February 22, 2019.